Anti-human Activin Receptor-like Kinase 1 (ALK1) Antibody Attenuates Bone Morphogenetic Protein 9 (BMP9)-induced ALK1 Signaling and Interferes with Endothelial Cell Sprouting*

Laurens A. van Meeteren[‡1], Midory Thorikay[‡], Simon Bergqvist[§], Evangelia Pardali[¶], Corrado Gallo Stampino[||],
Dana Hu-Lowe[§], Marie-José Goumans[‡], and Peter ten Dijke[‡2]

From the [‡]Department of Molecular Cell Biology and Centre for Biomedical Genetics, Leiden University Medical Center,
Postzone S-1-P, Postbus 9600, 2300 RC Leiden, The Netherlands, [§]Oncology Research Unit, Pfizer Inc., San Diego, California 92121,
[¶]Department of Cardiology and Angiology, University of Münster, 48149 Münster, Germany and [||]Clinical Oncology, Pfizer Italia Srl,
20152 Milan, Italy

Background: ALK1 is a TGF-β receptor essential for angiogenesis. An anti-ALK1 antibody is being tested in clinical trials as an inhibitor for tumor angiogenesis.
Results: Anti-hALK1 antibody selectively recognizes ALK1 and interferes with ALK1 ligand binding, signaling, and endothelial sprouting.
Conclusion: Anti-hALK1 antibody is a function-blocking antibody that prevents ALK1 signaling.
Significance: This study shows mechanistically how anti-hALK1 antibody exerts its effect on angiogenesis.

Genetic and molecular studies suggest that activin receptor-like kinase 1 (ALK1), a transforming growth factor β (TGF-β) type I receptor, and endoglin, a TGF-β co-receptor, play an essential role in vascular development and pathological angiogenesis. Several agents that interfere with ALK1 and endoglin function are currently in clinical trials for antiangiogenic activity in cancer therapy. One of these agents, PF-03446962 (anti-hALK1 antibody), shows promising results in the clinic. However, its effects on endothelial cell function and mechanism of action are unclear. Here we demonstrate that anti-hALK1 antibody selectively recognizes human ALK1. The anti-hALK1 antibody interfered with bone morphogenetic protein 9 (BMP9)-induced signaling in endothelial cells. Consistent with this notion, anti-hALK1 antibody was found to compete highly efficiently with the binding of the ALK1 ligand BMP9 and TGF-β to ALK1. Moreover, it prevented BMP9-dependent recruitment of co-receptor endoglin into this angiogenesis-mediating signaling complex. In addition, we demonstrated that anti-hALK1 antibody inhibited endothelial cell sprouting but did not directly interfere with vascular endothelial growth factor (VEGF) signaling, VEGF-induced proliferation, and migration of endothelial cells. Finally, we demonstrated that BMP9 in serum is essential for endothelial sprouting and that anti-hALK1 antibody inhibits this potently. Our data suggest that both the VEGF/VEGF receptor and the BMP9/ALK1 pathways are essential for stimulating angiogenesis, and targeting both pathways simultaneously may be an attractive strategy to overcome resistance to antiangiogenesis therapy.

Most of the clinically used antiangiogenesis therapies to date focus on interfering with the signal transduction cascade of vascular endothelial growth factor (VEGF) or basic fibroblast growth factor (bFGF)[3] (1). However, many studies have revealed that there are other growth factors that are equally essential for vascular development and function. One of these secreted classes of cytokines is the transforming growth factor β (TGF-β) family, which includes TGF-β, bone morphogenetic proteins (BMPs), and activins (2). The proangiogenic effects of several members of this family are mediated via the type I receptor activin receptor-like kinase 1 (ALK1) (3). Upon ligand binding, ALK1 forms a complex with type II serine/threonine kinase receptors, and ALK1 is phosphorylated by the type II receptor. Subsequently, ALK1 phosphorylates the transcription factors Smad1, -5, and -8, leading to the expression of proangiogenic genes like Id1 (4).

The expression of ALK1 is found to overlap with, but is not limited to, sites of angiogenesis and vasculogenesis in the developing mouse (5, 6). After birth, expression of ALK1 in vessels is suppressed but is induced again during neoangiogenesis in wound healing or in tumors (7). ALK1 knock-out embryos die at midgestation (around E11.5) due to severe vascular abnormalities such as hyperdilation of large vessels and large shunts

---

between arteries and veins. Furthermore, defects in recruitment and differentiation of supporting cells such as vascular smooth muscle cells are found (8, 9). Endothelial cell-specific knock-out mice show a phenotype similar to that of the full knock-out, indicating that the first critical role ALK1 has is in the endothelial cell for proper development of the vascular system (10). ALK1 is also important for lymphatic development because blockade of ALK1 signaling results in defective lymphatic development in multiple organs of neonatal mice (11). Zebrafish with a mutation in the ALK1 gene violet beauregarde suffer from an abnormal circulation pattern in which blood flows through a limited number of dilated cranial vessels and a failure to perfuse the trunk and tail (12).

In addition, the importance of ALK1 for the vascular system has been revealed by the identification of mutations in *ALK1* in hereditary hemorrhagic telangiectasia. Hereditary hemorrhagic telangiectasia is a familial human vascular syndrome that is characterized by cutaneous telangiectasias, increasingly severe nosebleeds, arterial venous malformations, and gastrointestinal hemorrhage (13).

Endoglin is a co-receptor for ALK1, and genetic studies have revealed many similarities between ALK1 and endoglin deficiency because endoglin mutations in humans also result in hereditary hemorrhagic telangiectasia (14). ALK1 and endoglin have been shown to engage in a complex, although whether this is ligand-dependent or -independent is debated (15, 16).

ALK1 could be a valuable target in antiangiogenesis therapy because of its specific expression in endothelial cells (17). Clinical phase I studies are currently being carried out with ALK1-Fc, a soluble chimeric protein consisting of the extracellular part of ALK1 fused to a Fc fragment (39) (ClinicalTrials.gov Identifier NCT 00996957). In mice that were orthotopically implanted with metastatic breast cancer cells (MCF7), ALK1-Fc treatment led to a 70% reduction in tumor burden (18). In the RIP1-Tag2 model for pancreatic cancer, which is highly dependent on the angiogenic switch in the tumors in a specific stage, it was shown that treatment with ALK1-Fc reduced tumor growth and progression due to reduced tumor angiogenesis. A similar phenotype was observed in RIP1-Tag2; ALK$^{+/-}$ mice, showing the specificity of the treatment (19).

PF-03446962, from now on denoted as anti-hALK1 antibody, is a monoclonal anti-human ALK1 antibody that recognizes the extracellular domain of ALK1 (40). It was generated by immunizing the human immunoglobulin G (IgG) 2 transgenic XenoMouse, resulting in a fully human monoclonal antibody (20). Previous studies showed that the antibody potently binds to cellular human ALK1 with a K_d of 7 nM. In a human/mouse chimera tumor model, the anti-hALK1 antibody decreased human vessel density and improved antitumor efficacy when combined with bevacizumab (anti-VEGF) (21).

The anti-hALK1 antibody is currently in phase I clinical trials (ClinicalTrials.gov Identifier NCT 00557856). Patients with advanced malignancies were found to have increased numbers of ALK1-positive circulating endothelial cells (22). Preliminary evidence from the trial indicates that the anti-hALK1 antibody reduced the amount of these ALK1-positive circulating endothelial cells. Furthermore, the phase I trial conducted in 44 patients has shown that the anti-hALK1 antibody up to 10 mg/kg is well tolerated without serious adverse events. The most common side effects were transient thrombocytopenia and asymptomatic elevation of pancreatic enzymes. Preliminary data showed encouraging clinical activity; noteworthy partial responses were observed in three patients who have previously received antiangiogenic therapies (23).

Although it has been postulated that anti-ALK1 therapy may be complementary to anti-VEGF in cancer intervention, the molecular mechanism by which anti-hALK1 antibody functions has not been extensively elucidated; in particular, it is not clear how it prevents ALK1 signaling in the context of multiple proangiogenic factors and which of the ALK1 ligands (*e.g.* TGF-β and BMP9) play a role in this process. Whether anti-hALK1 antibody demonstrates any direct cross-reactivity to and/or indirect inhibition of other highly related ALKs in the TGF-β receptor family is unclear.

We now provide direct evidence that anti-hALK1 antibody selectively recognizes only human ALK1 and no other related ALKs. We showed that anti-hALK1 antibody inhibits BMP9-induced signaling in endothelial cells. In addition, we demonstrated that anti-hALK1 competes and prevents BMP9 and TGF-β binding to ALK1. By attenuating ligand binding to the receptor, the antibody prevents the receptor from engaging in a complex with its co-receptor endoglin and more importantly in downstream signaling. Finally, we observed that anti-hALK1 antibody inhibits endothelial cell sprouting induced by proangiogenic growth factors. Because anti-hALK1 antibody inhibited endothelial sprouting to an extent similar to that of anti-BMP9 antibody, we propose that the BMP9 in serum is essential for sprouting and that anti-hALK1 antibody prevents serum-derived BMP9 from activating ALK1.

EXPERIMENTAL PROCEDURES

Cell Culture—Human umbilical vein endothelial cells (HUVECs) (pooled from multiple donors) (Lonza) were cultured either in Medium 199 with Earle's salt and L-glutamine (Invitrogen), 20% fetal calf serum (FCS), heparin (LEO Pharma), bovine pituitary extract (Invitrogen), and penicillin/streptomycin or in endothelial cell growth medium (EGM2) (Lonza) on plates coated with 0.1% gelatin at 37 °C in 5% CO_2. HUVECs were used up to passage 8. Human embryonic kidney (HEK) 293T, African green monkey kidney COS-1 cells, and mouse embryonic endothelial cells (MEECs) were cultured in Dulbecco's modified Eagle's medium (DMEM) with 10% FCS and penicillin/streptomycin.

Immunoprecipitation and Western Blot Analysis—COS-1 cells, HEK293T cells, or MEECs were transfected with the indicated plasmids using Lipofectamine according to the manufacturer's protocol (Invitrogen). Forty-eight hours after transfection, cells were lysed with immunoprecipitation buffer (20 mM Tris-HCl, pH 7.4, 150 mM NaCl, 1% Triton X-100, 10% glycerol, and protease inhibitor mixture (Roche Applied Science)). 1 μl of monoclonal anti-hemagglutinin (HA) (12CA5) or PF-03446962 antibody was used to immunoprecipitate ALK proteins for 3 h at 4 °C followed by precipitation with protein A-Sepharose beads. Beads were washed three times in immunoprecipitation buffer before 1× Laemmli sample buffer was added. Samples were subsequently subjected to sodium dodecyl sulfate-polyacryl-

amide gel electrophoresis (SDS-PAGE) and Western blotting. For total cell lysates, cell were lysed in radioimmune precipitation assay buffer (50 mM Tris-HCl, pH 7.2, 250 mM NaCl, 2% Nonidet P-40, 2.5 mM EDTA, 0.1% SDS, 0.5% sodium deoxycholate, and protease inhibitor mixture (Roche Applied Science)). Protein concentration was quantified by detergent-compatible (DC) protein assay (Bio-Rad). Lysates were subjected to SDS-PAGE and Western blotting.

HUVECs were serum-starved in endothelial basal medium (Lonza) for 4 h in the presence of anti-hALK1 antibody or control human IgG. For experiments with the blocking anti-BMP9 antibody (human/mouse BMP9 mAb, Clone 360107, R&D Systems), fetal calf serum and anti-BMP9 antibody at a final concentration of 0.5 μg/ml were premixed 30 min before adding to the cells. Subsequently, cells were stimulated with the indicated growth factors for the indicated time after which cells were washed with ice-cold phosphate-buffered saline (PBS) and lysed in radioimmune precipitation assay buffer. Lysates were subjected to SDS-PAGE and Western blotting.

Smad phosphorylation was detected with an antibody that specifically recognizes phosphorylated Smad1 (PS1 antibody) (24). The anti-Id1 antibody was from Santa Cruz Biotechnology. p38 and ERK phosphorylation was detected with phospho-specific antibodies from Cell Signaling Technology. Equal loading was shown with an anti-GAPDH antibody (Millipore).

Luciferase Reporter Assay—MEECs were transfected using Lipofectamine with pGL3(BRE)-luc (25) and β-gal construct to act as internal transfection control. After 36 h, cells were serum-starved overnight and treated with ligands. Luciferase activity was determined after 6 h of stimulation.

Constructs—Constructs encoding HA epitope-tagged ALK proteins were a kind gift from Dr. Eiichi Oeda and have been described previously (26). Human endoglin was expressed with a C-terminal FLAG tag from the pDEF3-hEndoglin-FLAG plasmid and was a kind gift from Dr. Susumu Itoh.

shRNA-mediated Depletion of ALK1—HUVECs were infected with lentivirus encoding an shRNA sequence against human ALK1 (TRCN0000000354, TRCN0000000355, and TRCN0000000356) selected from the MISSION shRNA library (Sigma). As a control, a non-targeting shRNA sequence was used (SHC002) (Sigma). Virus transduction was performed overnight, and the infected cells were selected using culture medium containing puromycin (1 μg/ml) for 48 h. Thereafter, the selected cells were processed for flow cytometry analysis. Three independent shRNA sequences were tested, and knockdown was verified by qPCR.

Flow Cytometry—HUVECs or COS-1 cells were incubated with PBS-EDTA to obtain single cell solutions. Cell suspensions were incubated on ice in 10% FCS for 30 min and subsequently stained with 1 μg of antibody/$\sim$1 $\times$ 10^6 cells. Primary antibody staining was followed by secondary staining using goat anti-human Alexa Fluor 488 (Invitrogen). Stained cells were analyzed by FACS (BD LSR II FACS analyzer) using FACSDiva software.

Endothelial Sprouting Bead Assay—A fibrin gel assay was performed as described previously (27, 28). In brief, 10^6 HUVECs were incubated with 2.5 $\times$ 10^3 Cytodex 3 microcarrier beads (Sigma-Aldrich) in EGM-2 for 4 h in a FACS tube

with gentle shaking every 30 min. Afterward, the bead solution was collected, transferred to a T25 flask, and incubated overnight at 37 °C in 5% CO$_2$. The following day, fibrinogen (Sigma-Aldrich) was dissolved in serum-free EGM-2 to a final concentration of 2 mg/ml and passed through a 0.22-μm syringe filter before being combined with the HUVEC-coated beads (300 beads/ml) and aprotinin solution at 0.15 unit/ml. For each condition, 0.63 μl of a 50 units/ml thrombin solution (Sigma-Aldrich) was added to the center of each well in a 48-well plate, and 0.25 ml of the fibrinogen solution was mixed with the thrombin-spotted wells. The fibrinogen-bead solution was allowed to clot for 5 min at room temperature followed by 15 min at 37 °C in 5% CO$_2$. Following polymerization, fully supplemented EGM-2 alone or with 25 ng/ml VEGF and antibodies at a final concentration of 40 μg/ml were added. On top of the clot, human fibroblasts were seeded at a concentration of 10^3 cells/well.

Endothelial Sprouting Spheroid Assay—Spheroids (750 cells/well) were prepared by culturing HUVECs in complete medium containing 0.1% methylcellulose. The next day, spheroids were collected and embedded in a collagen type 1 matrix and incubated with 50 ng/ml recombinant human VEGF (R&D Systems).

^{125}*I-BMP9 Binding Assay*—Iodination of BMP9 was performed according to the chloramine T method, and cells were subsequently affinity-labeled with the radioactive ligand as described before (29, 30). In brief, cells were incubated on ice for 2 h with the radioactive ligand. After incubation, cells were washed, and cross-linking was performed using 54 mM disuccinimidyl suberate and 3 mM bis(sulfosuccinimidyl)suberate (Pierce) for 15 min. Cells were washed, scraped, and lysed. Lysates boiled in SDS sample buffer and subjected to SDS-PAGE directly or were incubated with anti-ALK1 (9, 31) overnight, and immune complexes were precipitated by adding protein A-Sepharose (Amersham Biosciences). Samples were washed, boiled in SDS sample buffer, and subjected to SDS-PAGE. Gels were dried and scanned with the Storm imaging system (Amersham Biosciences).

Epitope Mapping—Epitope mapping of anti-hALK1 was carried out by ELISA using an overlapping peptide library based on the human ALK1 extracellular domain (ECD) sequence (residues 22–118). Peptides were 15 amino acids in length with an overlap of 4 residues. Peptides were synthesized on a 100-nmol scale and contained a C-terminal glycine residue (JPT Peptide Technologies, Berlin, Germany).

Surface Plasmon Resonance—The ALK1-anti-hALK1 antibody surface plasmon resonance studies were carried out using a Biacore 3000(GE Healthcare) at 25 °C in 150 mM NaCl, 25 mM HEPES, pH 7.5, 2 mM MgCl$_2$, 0.005% P20 surfactant. Human ALK1 (R&D Systems catalog number 370-AL) was immobilized by standard amine coupling on a carboxymethylated dextran CM5 sensor chip. BMP9 binding was measured using 40 nM human BMP9 (R&D Systems catalog number 3209-BP). BMP9 competition studies were carried out using 50 nM anti-hALK1 or 50 nM anti-human ALK1 polyclonal antibody (R&D Systems catalog number AF370). Free ALK1 was regenerated using a 1-min pulse of 100 mM H$_3$PO$_4$ between injection cycles. Injections were referenced to an unmodified flow cell surface, and

data analysis was performed using Scrubber2 software (Bio-Logic Software, Pty., Australia).

Cell Growth and Migration Assays—HUVECs were seeded at a density of 3×10^3 cells/well in 96-well plates. The next day, medium was aspirated and replaced by fresh medium containing the respective ligands. Proliferation of cells was determined after 2 and 3 days by adding 3-(4,5-dimethylthiazol-2-yl)-5-(3-carboxymethoxyphenyl)-2-(4-sulfophenyl)-2*H*-tetrazolium solution (Promega) and measuring the absorbance at 490 nm. Migration of HUVECs was measured in 48-well Boyden chambers (Neuroprobe). Filters (8-μm pores) were coated with collagen overnight, and cells were grown in low serum (1%) endothelial basal medium overnight, trypsinized, and seeded in the upper chamber. After 5 h, cells at the top side were removed, and migrated cells at the bottom side of the filter were fixed and stained. Stained filters were scanned and quantified. All measurements were done in quadruple. Representative experiments are shown.

qPCR—RNA was isolated using the NucleoSpin RNA II kit according to the manufacturer's protocol (Bioké, Leiden, The Netherlands). cDNA was produced from 1 μg of RNA with the RevertAid H-Minus First Strand cDNA Synthesis kit (Fermentas) using oligo(dT) primers. The qPCR was performed with 2 μl of 12× diluted cDNA, 4 μl of 2× FastStart Universal SYBR Green Master Mix (Roche Applied Science), and 750 nM forward and reverse primers in a total volume of 8 μl. Amplification was done on a LightCycler 480 (Roche Applied Science) according to the following PCR protocol: initial denaturation of 10 min at 95 °C; 45 cycles of denaturation at 95 °C for 10 s, annealing at 60 °C for 30 s, and amplification at 72 °C for 20 s; and final elongation for 5 min at 72 °C followed by a melting curve program. The primers used were as follows: human ALK1: forward, 5′-atgacctcccgcaactcga-3′; reverse, 5′-tagagggagccgtgctcgt-3′; VEGF-R2: forward, 5′-aaagggtggaggtgactgag-3′; reverse, 5′-cggtagaagcacttgtaggc-3′; and COX-2: forward, 5′-tcacgcatcagtttttcaaga-3′; reverse, 5′-tcaccgtaaatatgatttaagt-ccac-3′. Transcripts were analyzed with the household gene *GAPDH* as the reference gene.

RESULTS

Anti-hALK1 Antibody Selectively Recognizes ALK1—ALK1 is a member of a family of seven TGF-β type I serine/threonine kinase receptors. ALKs share a varying degree of homology and have diverse, sometimes even opposite, biological effects upon activation (32). Therefore, a therapeutic antibody against ALK1 should have no cross-reactivity to the other family members. We tested the specificity of the anti-hALK1 antibody against other ALKs including the highly related ALK2. cDNA encoding HA-tagged human ALK1, ALK2, ALK3, ALK4, ALK5, or rat ALK7 was transfected in COS-1 cells. Samples were lysed, and expression was confirmed by Western blotting for the HA epitope tag (Fig. 1*A*, *third panel*). Subsequently, we tested the ability of the anti-hALK1 antibody to immunoprecipitate HA epitope-tagged ALKs in cell lysates of transfected cells and used HA antibody immunoprecipitation as a control. As expected, all ALKs were immunoprecipitated with the anti-HA antibody (Fig. 1*A*, *upper panel*). Only ALK1 was successfully immunoprecipitated by anti-hALK1 antibody. Other ALKs including

the most closely related ALK2 were not immunoprecipitated by the anti-hALK1 antibody (Fig. 1*A*, *second panel*). Moreover, mouse ALK1, which shares 75% identity with human ALK1 in its extracellular domain, was not recognized by anti-hALK1 antibody (data not shown). When we incubated the blot with the anti-hALK1 antibody, we were unable to detect ALK1 or any of the other ALKs (Fig. 1*A*, *fourth panel*), indicating that the anti-hALK1 antibody is not suited for recognition of ALK1 in Western blot.

Next, we tested whether the anti-hALK1 antibody recognizes human ALK1 when expressed on the surface of live cells using flow cytometric analysis. Because endothelial cells are known to express ALK1, we incubated HUVECs with the anti-hALK1 antibody and performed flow cytometry. HUVECs stained positive for ALK1 when compared with HUVECs that were incubated with an isotype-matched control antibody (Fig. 1*B*, *left panel*). To further confirm that the anti-hALK1 antibody indeed recognized only human ALK1 on the surface of the cells, we depleted HUVECs of human ALK1 by transduction with a lentivirus expressing either a nonspecific shRNA or a specific shRNA sequence to knock down ALK1 expression. HUVECs were selected for shRNA expression using puromycin, and ALK1 depletion was confirmed by qPCR analysis (data not shown). Flow cytometric analysis showed that the ALK1 knockdown cells no longer stained positive using the anti-hALK1 antibody (Fig. 1*B*, *middle panel*). In addition, COS-1 cells transfected with a human ALK1 plasmid stained positive in flow cytometry analysis using anti-hALK1 antibody, whereas mock-transfected cells did not (Fig. 1*B*, *right panel*).

Subsequently, we mapped an epitope in the extracellular domain of ALK1 to a peptide that is recognized by the anti-hALK1 antibody. With an overlapping peptide library of 15-mers with a 4-residue overlap, we mapped the epitope to residues 42–56 (KGPTCRGAWCTVVLV) of the human ALK1 ECD (Fig. 1*C*). This region of ALK1 shares little homology to other ALK receptors, which could explain why anti-hALK1 shows no cross-reactivity to other ALK receptors.

Anti-hALK1 Antibody Blocks BMP9-induced Signaling in Endothelial Cells—ALK1 is a high affinity receptor for BMP9, and upon BMP9 binding, ALK1 phosphorylates Smad1 and Smad5, resulting in induction of Id1 expression (31). Therefore, we tested whether anti-hALK1 antibody interferes with BMP9/ALK1-induced responses. HUVECs were serum-starved for 4 h and subsequently stimulated with VEGF, bFGF, TGF-β, BMP9, or FCS in the presence of anti-hALK1 antibody or a control IgG. Subsequently, phospho-Smad1/5 or Id1 expression was measured by Western blot analysis after 30 min. BMP9, but not VEGF or bFGF, induced pSmad1 and Id1 expression. FCS that contains BMP9 (33) is also capable of mediating this response. Both the BMP9- and FCS-induced responses were potently inhibited by anti-hALK1 antibody (Fig. 2*A*). In addition, the effect of the anti-hALK1 antibody on the kinetics of BMP9-induced pSmad1 activation was tested. Both BMP9-induced intensity and duration of Smad1 phosphorylation were mitigated (Fig. 2*B*).

To measure downstream ALK1 responses, we used a BMP-responsive element (BRE)-luciferase reporter. MEECs that do not express ALK1 endogenously were transfected with mock or
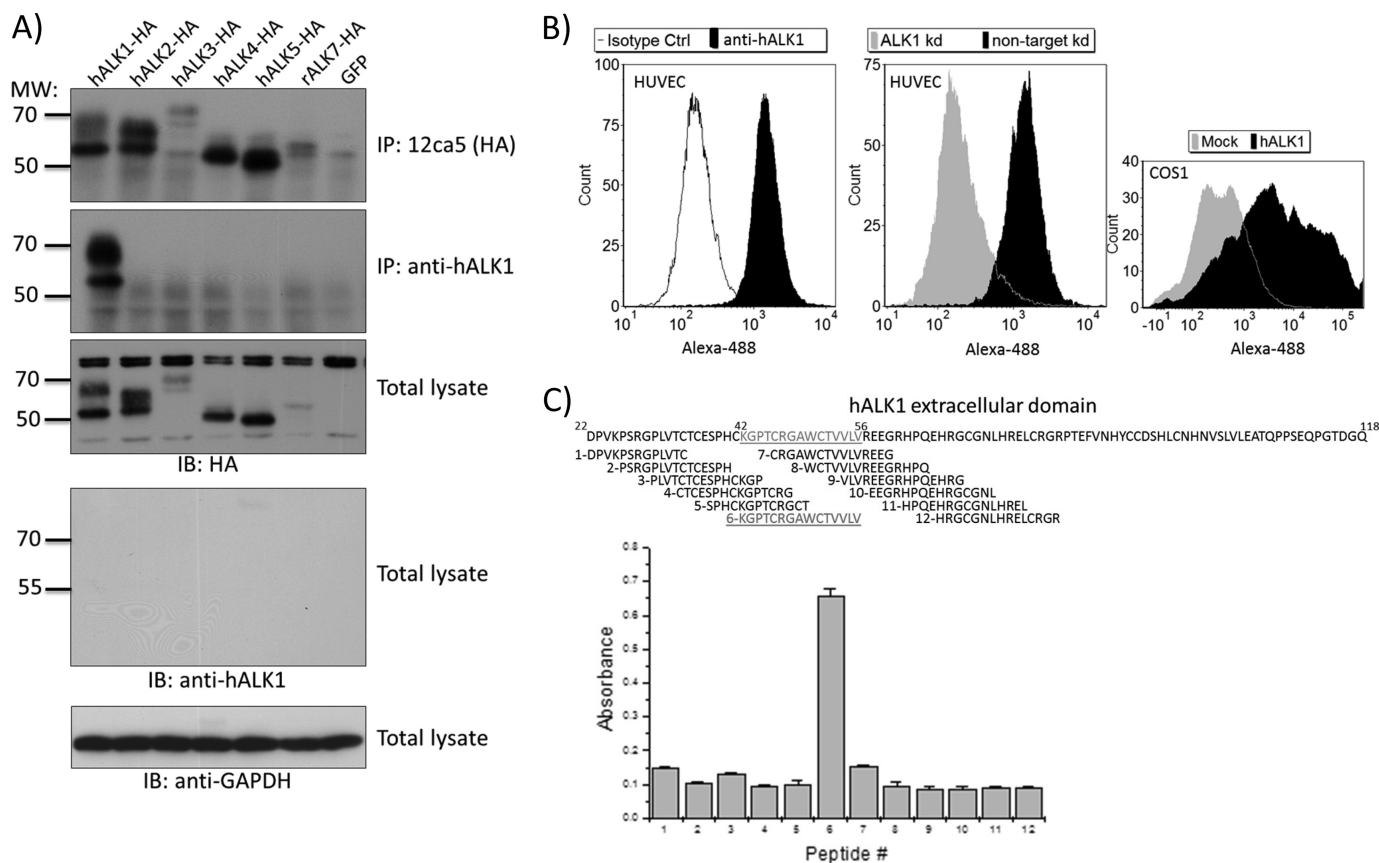
FIGURE 1. **Anti-hALK1 antibody selectively recognizes human ALK1.** *A*, COS-1 cells were transfected with plasmids encoding human ALK1-HA, human ALK2-HA, human ALK3-HA, human ALK4-HA, human ALK5-HA, rat ALK7-HA, or GFP, respectively. The *upper panel* shows that all ALKs were expressed, although ALK3 and ALK7 were expressed at a lower level. After lysis, immunoprecipitation (*IP*) was performed with either 12CA5 (*second panel*) or anti-hALK1 (*third panel*). Thereafter, immunoprecipitates were subjected to SDS-PAGE and then blotted with anti-HA antibody. Whereas 12CA5 (anti-HA) was able to immunoprecipitate all the different HA-tagged ALKs, anti-hALK1 antibody only specifically immunoprecipitated ALK1. The *fourth panel* shows total lysates blotted with the anti-hALK1 antibody, which showed no signal, indicating that anti-hALK1 antibody does not work in Western blotting. For a loading control, the cell lysates were analyzed for GAPDH expression (*bottom panel*). *B*, *left panel*, HUVECs were stained with anti-hALK1 antibody or isotype control (*Ctrl*) antibody followed by a secondary anti-human Alexa Fluor 488 antibody and subsequently analyzed by flow cytometry. *Middle panel*, HUVECs were treated with lentivirus expressing an shRNA to knock down hALK1 or a non-targeting control shRNA. Subsequently, cells were analyzed by flow cytometry using anti-hALK1 antibody. A clear reduction in staining can be seen. Similar results were obtained by a second independent ALK1 knockdown (*kd*) shRNA construct, and reduction in ALK1 expression was also verified by qPCR (data not shown). *Right panel*, COS-1 cells were transfected with a plasmid encoding human ALK1 or a control mock plasmid. After transfection, cells were analyzed by flow cytometry using anti-hALK1 antibody and a secondary anti-human Alexa Fluor 488 antibody. The intensity of the Alexa Fluor 488 signal is plotted on the *x axis* against the number of cells (*count*) on the *y axis*. *C*, epitope mapping of anti-hALK1 was carried out by ELISA using an overlapping peptide library based on the human ALK1 ECD sequence (residues 22–118). Peptides were 15 amino acids in length with an overlap of 4 residues. Anti-hALK1 recognized a single peptide corresponding to residues 42–56 (KGPTCRGAWCTVVLV) of the human ALK1 ECD. Plotted are absorbance values ± S.D. (*n* = 5). *IB*, immunoblot.

human ALK1 together with the BRE-luciferase reporter construct. After overnight serum starvation, cells were stimulated with BMP9, FCS, or TGF-β in the presence of a control IgG or anti-hALK1. Both BMP9 and FCS induced a potent luciferase response only in cells transfected with human ALK1 that was blocked by anti-hALK1. TGF-β, although reported to weakly induce BRE-luciferase, did not give any significant induction above unstimulated conditions (Fig. 2*C*).

BMP9 Binding to ALK1 Is Prevented by Anti-hALK1 Antibody—Because BMP9 signaling is blocked by anti-hALK1 antibody, we hypothesized that anti-hALK1 antibody competes directly with BMP9 for ALK1 binding. To test this, the human recombinant ECD of ALK1 was immobilized on a Biacore chip to study ALK1 binding by measuring surface plasmon resonance. High affinity binding of both BMP9 and anti-hALK1 antibody to the immobilized ALK1 was independently observed (Fig. 3*A*, *a*). However, when the immobilized ALK1

was presaturated with the anti-hALK1 antibody, no significant binding of BMP9 was observed, indicating that the anti-hALK1 antibody is able to block binding of BMP9 to ALK1 (Fig. 3*A*, *b*). BMP9 binding was only partially reduced in the presence of an anti-ALK1 polyclonal antibody (Fig. 3*A*, *c*). In addition, when ALK1 was presaturated with BMP9, binding of the anti-hALK1 antibody was observed in the surface plasmon resonance sensorgram but with a significantly reduced association rate compared with the free ALK1 interaction (Fig. 3*A*, *d*). The latter suggests an exchange of BMP9 for anti-hALK1 antibody on the recombinant ALK1 ECD. Together the results indicate that ALK1 cannot bind BMP9 and anti-hALK1 simultaneously and that the antibody and ligand compete for ALK1 binding.

To test whether the anti-hALK1 antibody has similar effects in endothelial cells, HUVECs were incubated with iodinated BMP9 in the presence of increasing concentrations of anti-hALK1 antibody or control IgGs (0.01–10 μg/ml). After a 2-h
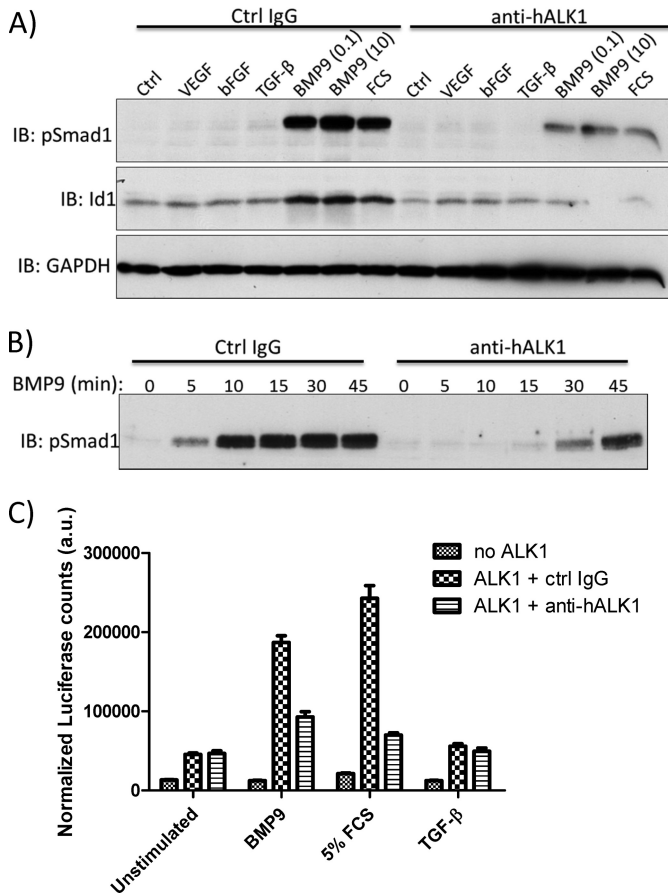
FIGURE 2. **Anti-hALK1 antibody inhibits BMP9-induced signaling in endothelial cells.** *A*, HUVECs were stimulated for 30 min with VEGF (20 ng/ml), bFGF (30 ng/ml), TGF-β (1 ng/ml), BMP9 (0.1 and 10 ng/ml), or FCS (3%) in the presence of anti-hALK1 antibody or a control IgG. Phospho-Smad1/5 and Id1 levels were measured by immunoblot (*IB*) analysis. BMP9 and FCS induced pSmad1 and Id1, and this response was potently inhibited by anti-hALK1 antibody treatment. *B*, HUVECs were stimulated with 0.1 ng/ml BMP9 in the presence of anti-hALK1 antibody or a control IgG. The kinetics of phospho-Smad1/5 signaling was measured by immunoblot analysis. The intensity and duration of BMP9-induced Smad1/5 phosphorylation were inhibited by anti-hALK1 antibody. *C*, MEECs were transfected with mock (no ALK1) or human ALK1 together with BRE-luciferase and CMV-β-galactosidase contructs. 36 h after transfection, cells were serum-starved overnight and subsequently stimulated for 6 h with BMP9 (1 ng/ml), FCS (5%), or TGF-β (5 ng/ml) in the presence of either a control (*ctrl*) IgG or anti-hALK1 antibody. Anti-hALK1 antibody inhibited the BMP9 and FCS induced luciferase response. *a.u.*, arbitrary units. Plotted are values ± S.E. ($n = 6$).

incubation on ice, BMP9 was chemically cross-linked. After gel electrophoresis, BMP9-bound complexes were identified by autoradiography. To identify ALK1-BMP9 complexes, ALK1 was immunoprecipitated from lysates of cells in which cell surface proteins were affinity-labeled with iodinated BMP9. The position where ALK1-BMP9 complex ran on the gel is indicated with an *arrow* in Fig. 3B. Anti-hALK1 antibody potently inhibited the formation of BMP9-ALK1 complexes at concentrations from 0.1 to 10 μg/ml. As can be seen in the quantification (Fig. 3B, *lower panel*), the anti-hALK1 potently inhibited the formation of the ALK1-BMP9 complex, consistent with the observed results from the Biacore experiments.

In addition, we overexpressed human and mouse ALK1 in COS-1 cells and performed a cross-linking experiment with BMP9 and TGF-β on these overexpressed proteins. GFP-transfected COS-1 cells did not show any radiolabeled cross-linked

proteins, indicating that BMP9 and TGF-β did not bind (Fig. 3C). Cells transfected with human ALK1 alone or together with BMP receptor type II potently bound BMP9, and a BMP9-ALK1 complex can be seen. This complex formation was effectively blocked by addition of the anti-hALK1 antibody. Transfected mouse ALK1 also effectively bound BMP9; however, the interaction between mouse ALK1 and BMP9 could not be blocked by the anti-hALK1 antibody, showing that the anti-hALK1 antibody has a human-selective blocking function (Fig. 3C). These data are in line with our data that anti-hALK1 antibody did not immunoprecipitate and recognize mouse ALK1 in flow cytometry (data not shown).

The interaction between TGF-β and ALK1 was dependent on the presence of the TGF-β type II receptor. Therefore, we co-transfected human ALK1 with TGF-β type II receptor. TGF-β bound specifically to ALK1, and this interaction could also be blocked by anti-hALK1 (Fig. 3C).

Because ALK1 is known to bind the co-receptor endoglin upon ligand binding (15, 16), we subsequently examined the effect of anti-hALK1 antibody on ALK1-endoglin complex formation. In HEK293T cells, human ALK1-HA and human endoglin-FLAG were co-transfected (Fig. 3D). From the lysates, ALK1 was successfully precipitated (Fig. 3C, see *upper left panel*) either by an HA antibody (Fig. 3D, *second lane*) or by anti-hALK1 antibody (Fig. 3D, *third lane*). Subsequently, the blots were reprobed for co-immunoprecipitated endoglin-FLAG (Fig. 3D, *lower left panel*). Strikingly, although anti-HA and anti-hALK1 antibodies both immunoprecipitated equal amounts of ALK1, anti-hALK1 antibody failed to co-immunoprecipitate endoglin (Fig. 3D, *third lane*, *lower left panel*). The *right panels* show total lysates. The data support the notion that the anti-hALK1 antibody interferes with BMP9-induced ALK1-endoglin complex formation.

Anti-hALK1 Antibody Does Not Inhibit VEGF-induced Signaling, Migration, Proliferation, and Transcription—Given its role in angiogenesis, we checked whether anti-hALK1 had an effect on VEGF-induced signaling, migration, proliferation, or gene transcription. In HUVECs, VEGF induced a rapid activation of p38 and ERK. No effect of the anti-hALK1 antibody was seen on this induction (Fig. 4A). In addition, we tested the effect of anti-hALK1 on VEGF-induced migration in a Boyden chamber setup and on VEGF-induced proliferation. Whereas the VEGF inhibitor sunitinib blocked migration and proliferation, we did not find any effect of anti-hALK1 on these VEGF-induced processes (Fig. 4, B and C).

Finally, we measured angiogenic markers such as VEGF receptor 2 and COX-2, which are known to be transcriptionally activated by VEGF. Both the early induced expression of *VEGF-R2* (Fig. 4D) and the late induced expression of *COX-2* (Fig. 4E) were not affected by anti-hALK1, indicating that anti-hALK1 has no direct effect on the VEGF signaling cascade and gene transcription.

Anti-hALK1 Antibody Inhibits Endothelial Cell Sprouting—Given the involvement of ALK1 signaling in angiogenesis (3), we tested the effect of anti-hALK1 antibody in an endothelial cell sprouting assay. We seeded HUVECs on latex beads and embedded the HUVEC-coated beads in a fibrin gel with a top layer of supporting fibroblasts. Upon the addition of the
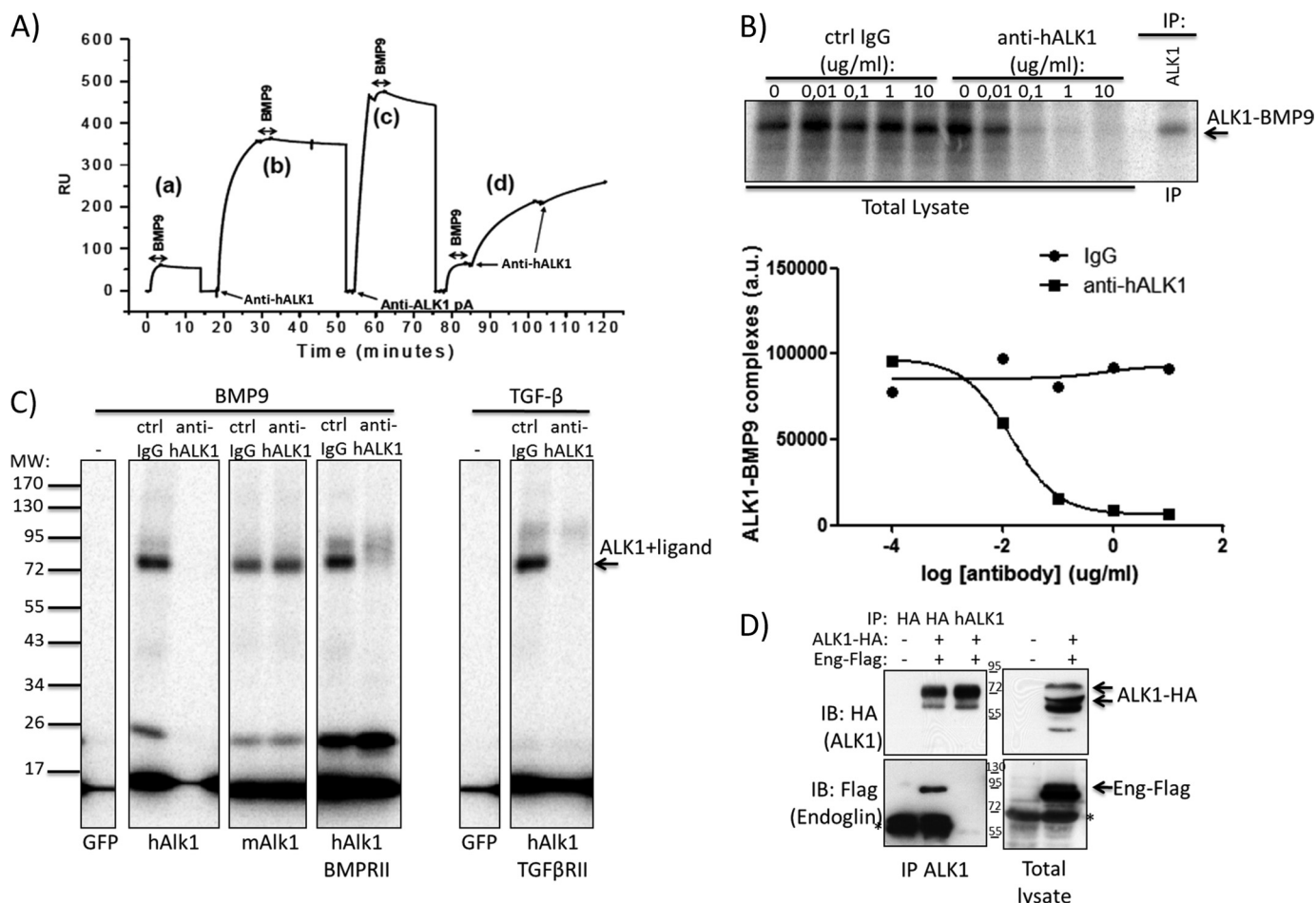
FIGURE 3. **Anti-hALK1 antibody competes with BMP9 for ALK1 binding and prevents heteromeric ALK1-endoglin complex formation.** *A*, human recombinant extracellular domain of ALK1 was immobilized on a Biacore chip to study ALK1 binding by measuring surface plasmon resonance. BMP9 bound immobilized recombinant ALK1 with high affinity (*a*). Anti-hALK1 antibody binding to recombinant hALK1 blocked BMP9 binding (*b*). BMP9 binding was partially reduced in the presence of an anti-ALK1 polyclonal antibody (*pA*) (*c*). When recombinant ALK1 surface was saturated with BMP9, anti-hALK1 antibody binding was observed (*d*) with a significantly reduced association rate. *RU*, relative units. *B*, ^{125}I-labeled BMP9 was added to HUVECs that were incubated with increasing concentrations of control (*Ctrl*) IgG or anti-hALK1 antibody (0.01–10 μg/ml). After a 2-h incubation on ice, BMP9 was chemically cross-linked to cell surface proteins. After gel electrophoresis, BMP9-bound complexes were identified by autoradiography. To identify ALK1-BMP9 complexes, ALK1 was immunoprecipitated (*IP*) from cell lysates. Anti-hALK1 antibody blocked the formation of BMP9-ALK1 complexes at concentrations from 0.1 μg/ml. Quantification of the ALK1-BMP9 band using ImageQuant software (Amersham Biosciences) is shown *below*. *a.u.*, arbitrary units. *C*, COS-1 cells were transfected with the indicated plasmids and subsequently incubated with ^{125}I-labeled BMP9 or TGF-β in the presence of a control IgG or anti-hALK1 (10 μg/ml). After a 2-h incubation on ice, BMP9 and TGF-β were chemically cross-linked to cell surface proteins. After gel electrophoresis, ligand-bound receptor complexes were identified by autoradiography. GFP-transfected cells did not bind BMP9 or TGF-β. Human ALK1, mouse ALK1, and the combination of human ALK1 and BMP type II receptor all bound BMP9. The interaction with human ALK1, but not mouse (*m*) ALK1, was inhibited by the addition of anti-hALK1. TGF-β binding to ALK1 was similarly blocked by addition of anti-hALK1. All panels come from the same gel and were exposed equally long. *D*, HEK293T cells were either mock- (*first lane*) or co-transfected with human ALK1-HA antibody and human endoglin-FLAG (*second* and *third lanes*). From lysates, ALK1 was successfully precipitated (see *upper left panel*) either by HA antibody (*second lane*) or by the anti-hALK1 antibody (*third lane*). Subsequently, blots were reprobed for co-immunoprecipitated endoglin-FLAG (*lower left panel*). Strikingly, although anti-HA and anti-hALK1 antibody both immunoprecipitated (*IP*) equal amounts of ALK1, anti-hALK1 antibody failed to co-immunoprecipitate endoglin (*Eng*). The *right panels* show control lysates of mock- (*first lane*) and co-transfected cells (*second lane*). Note that mature ALK1 (highest molecular mass) was favorably immunoprecipitated by both the HA and anti-hALK1 antibodies. *Numbers* indicate the molecular mass marker bands (in kDa), and * denotes nonspecific bands. *IB*, immunoblot.

endothelial cell medium EGM2 (2% FCS, EGF, hydrocortisone, VEGF, bFGF, insulin-like growth factor-1, ascorbic acid, and heparin (Lonza)) plus 25 ng/ml VEGF-A, endothelial cells sprouted from the bead, but upon adding anti-hALK1 antibody to the gel, sprouting was partially blocked (Fig. 5*A*).

Serum contains bioactive BMP9 (33); therefore, we investigated whether BMP9/ALK1 interaction mediated HUVEC sprouting. First, we checked whether the anti-hBMP9 antibody prevents FCS-induced ALK1 signaling. Indeed, anti-BMP9 neutralizing antibody prevented FCS-induced Smad1 phosphorylation and induction of Id1 expression (Fig. 5*B*). Second,

we tested anti-BMP9 in the endothelial sprouting assays. Anti-BMP9 potently inhibited endothelial sprouting to a level similar to that of anti-hALK1 antibody (Fig. 5*C*).

In this assay, fibroblasts are also present (on top of the layer), and the effects could also be explained by the effects the antibody has on the fibroblasts. Therefore, we tested anti-hALK1 and anti-BMP9 in a sprouting assay using only endothelial cells. Spheroids of HUVECs were embedded in collagen and stimulated with growth factor and serum-containing EGM2 plus VEGF in the presence of anti-hALK1 or anti-BMP9. Both antibodies inhibited endothelial sprouting to a similar extent (Fig. 5*D*).
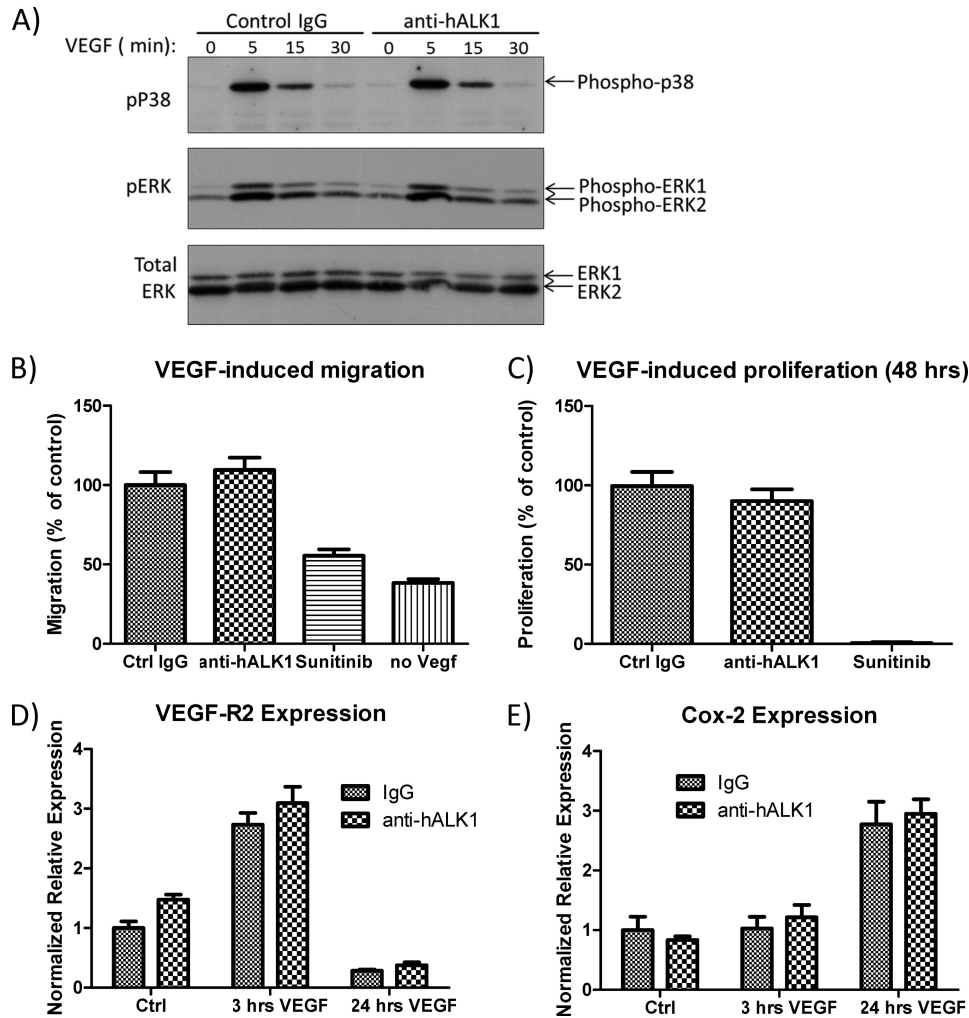
FIGURE 4. *A*, HUVECs were stimulated with VEGF in the presence of a control antibody or anti-hALK1 antibody. Anti-hALK1 antibody had no effect on p38 or on ERK activation by VEGF. Cell lysates were analyzed by Western blot. Phosphorylation of p38 (*pP38*) and ERK (*pERK*) was measured using phosphospecific antibodies. Total ERK levels in cell lysates are also shown. *B*, migration of HUVECs was measured in 48-well Boyden chambers (Neuroprobe). HUVECs were grown in low serum overnight and seeded on collagen-coated filters. The lower chamber contained medium with 1% serum, 25 ng/ml VEGF, and antibodies or sunitinib. After 5 h, cells at the top side were removed, and migrated cells at the bottom side of the filter were fixed and stained. Stained filters were scanned and quantified. All measurements were done in quadruplicate. Plotted are values ± S.E. (*n* = 4) relative to the values of control that was set at 100%. Anti-hALK1 antibody had no effect on VEGF-induced migration, whereas the VEGF inhibitor sunitinib did. *C*, HUVECs were stimulated for 48 h with 1% FCS and 25 ng/ml VEGF-A in the presence of control (*Ctrl*) IgG, anti-hALK1 antibody (both at 40 μg/ml), or sunitinib (25 nM). Proliferation was measured by CellTiter AQueous One Solution Cell Proliferation Assay (Promega). Plotted are values ± S.E. (*n* = 4) relative to the values of control that was set at 100%. The addition of anti-hALK1 antibody had no effect on VEGF-induced proliferation, whereas sunitinib potently inhibited VEGF-induced proliferation. *D* and *E*, HUVECs were serum-starved for 4 h in the presence of control IgG or anti-hALK1 and subsequently stimulated with 10 ng/ml human VEGF-A. RNA was isolated before, 3 h after, and 24 h after start of stimulation. *VEGF-R2* (*D*) and *COX-2* (*E*) expression levels were determined. Plotted are values ± S.E. (*n* = 3). Anti-hALK1 did not affect VEGF-induced gene expression of these genes.

DISCUSSION

Here we report that anti-hALK1 antibody, an antibody in clinical trials, prevents BMP9 binding to ALK1 and subsequently leads to inhibition of endothelial cell organization. We show that anti-hALK1 is specific for human ALK1 and has no cross-reactivity to any of the other highly related ALKs or to mouse ALK1. Anti-hALK1 antibody inhibits BMP9-induced Smad1 phosphorylation and Id1 expression. Experiments using radiolabeled BMP9 and Biacore analysis showed that BMP9 binding to ALK1 is inhibited by anti-hALK1 antibody. In addition, anti-hALK1 also interfered with ALK1/TGF-β interaction. Anti-hALK1 antibody inhibited endothelial cell sprouting by inhibiting serum-derived BMP9 signaling. Anti-hALK1 antibody does not inhibit endothelial cell sprouting by interfering

with direct VEGF signaling because we did not find any effect of anti-hALK1 antibody on direct VEGF-induced signaling responses and VEGF-induced migration and proliferation. In addition, VEGF-induced VEGF receptor tyrosine phosphorylation was also not affected (data not shown). Because BMP9 is reported to be a proangiogenic factor (34), our results give a mechanistic explanation for the effects of this antibody on angiogenesis.

Interestingly, we mapped the binding site of anti-hALK1 to residues 42–56 (KGPTCRGAWCTVVLV) of the human ALK1 ECD. In a model of the ALK1, the structure of this region was predicted to contain several residues involved in the ALK1/BMP9 interaction (35).

BMP9 has been described as an inhibitor of endothelial cell proliferation. However, one must note that in these studies
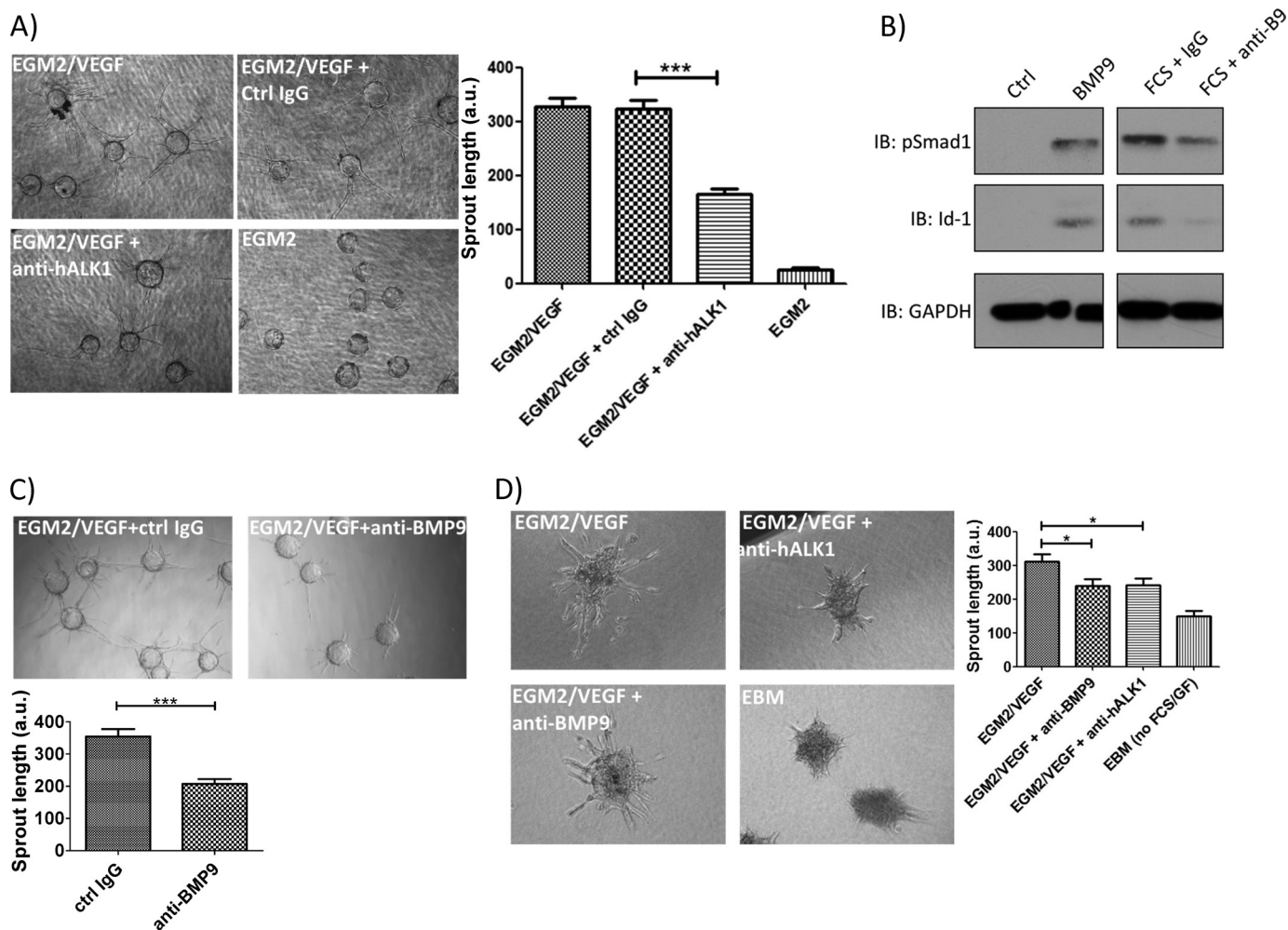
FIGURE 5. **Anti-hALK1 antibody inhibits endothelial cell sprouting.** *A*, endothelial cells were coated on beads and embedded in a fibrin gel on top of a layer of supporting fibroblasts. Upon the addition of EGM2 plus VEGF, endothelial cells sprouted from the beads, and this effect was efficiently blocked by anti-hALK1 antibody (40 μg/ml). Plotted are mean values $\pm$ S.E. (***, $p < 0.001$). The absence of VEGF resulted in a total block of sprouting. *a.u.*, arbitrary units. Representative pictures are shown. *B*, HUVECs were stimulated for 35 min with BMP9 or 3% FCS. FCS was mixed with anti-BMP9 or a control IgG (both at a final concentration of 5 μg/ml) 30 min before addition to the cells. Phospho-Smad1 or Id1 signaling was measured by immunoblot (*IB*) analysis. FCS-induced pSmad1/5 and Id1 were inhibited by anti-BMP9 antibody. *C*, as in *A* but now in the presence of 5 μg/ml anti-BMP9 or control (*Ctrl*) IgG. The anti-BMP9 antibody inhibited endothelial sprouting. Plotted are mean values $\pm$ S.E. (***, $p < 0.001$). Representative pictures are shown. *D*, HUVEC spheroids were seeded in collagen, and endothelial basal medium (*EBM*) or the proangiogenic medium containing EGM2 plus VEGF was added together with anti-hALK1 or anti-BMP9 antibody. After 18 h, sprouting was evaluated. Both the anti-BMP9 and the anti-hALK1 antibodies blocked sprouting to a similar extent. Plotted are mean values $\pm$ S.E. (*, $p < 0.05$). Representative pictures are shown.

BMP9 was used at very high concentrations (10 ng/ml and higher), whereas BMP9 has an EC_{50} value of 50 pg/ml for ALK1 (31, 33, 36). Studies with a lower concentration of BMP9 actually show an opposing effect: BMP9 induced the proliferation of *in vitro*-cultured mouse embryonic stem cell-derived endothelial cells (34). Furthermore, *in vivo* angiogenesis was promoted by BMP9 in a Matrigel plug assay and in a BxPC3 xenograft model of human pancreatic cancer (34). A possible explanation lies in the fact that BMP9 may bind other receptors at higher concentrations that could have opposing effects on angiogenesis (37). Although the concentration of circulating BMP9 was reported to vary between 2 and 12 ng/ml in sera and plasma from healthy humans (33), the concentration of BMP9 in the proangiogenic tumor microenvironment is currently not known.

In endothelial cells, we saw little to no binding of radiolabeled TGF-β, and therefore, we could not assess in these endothelial cells whether anti-hALK1 antibody prevented the TGF-β/ALK1 interaction. Therefore, we used an overexpression system artificially overexpressing human ALK1 in the presence of TGF-β receptor type II. In this setup, we could measure TGF-β/ALK1 interaction, and this was potently blocked by the anti-hALK1. When human ALK1 was overexpressed in mouse endothelial cells, we did not observe any ALK1-induced BRE-luciferase activity upon stimulation with TGF-β. Therefore, we could not address whether anti-hALK1 blocks TGF-β/ALK1 signaling.

As indicated in the Introduction, both a ligand trap, the ALK1-Fc (18), and the anti-hALK1 antibody are currently being tested in clinical trials as antiangiogenesis agents. The biggest difference between these two approaches is that the ligand trap will scavenge all ALK1 ligands, thereby also preventing the binding of BMP9 to other receptors, which could ultimately lead to stimulation of angiogenesis by also inhibiting the

antiangiogenic activity of BMP9. Studies reporting that ALK1-Fc is proangiogenic (38) could possibly be explained by this mechanism. Therefore, we hypothesize that inhibiting the ALK1/BMP9 interaction specifically, as we show here that anti-hALK1 antibody does, may yield a more favorable clinical safety profile.

Our results give a unique insight into the mechanism for how anti-hALK1 antibody interferes with ALK1 function. By competing with ligand (BMP9) binding for ALK1, anti-hALK1 antibody prevents activation of ALK1 and intracellular downstream signaling responses including Smad1/5 phosphorylation and induction of Id1 expression. BMP9-induced ALK1 activation may also induce non-canonical Smad pathways that participate in endothelial cell organization; these responses will also be blocked by the anti-hALK1 antibody.

Interestingly, the anti-hALK1 antibody demonstrated inhibitory effects of endothelial cell sprouting in two different assays. These assays are dependent on the presence of both serum-derived BMP9 and VEGF. However, because we found no negative effect of anti-hALK1 on direct VEGF signaling, we suggest that the BMP9/ALK1 and the VEGF pathways are parallel pathways that do not converge on a receptor or direct intracellular signaling level. Our results indicate a co-requirement for these parallel pathways in angiogenesis and strengthen the notion that it will be beneficial to combine antiangiogenesis therapy targeting VEGF and ALK1. It is tempting to speculate that by combining these two approaches it will be less likely that resistance to the therapy, as is observed now with anti-VEGF therapy, will occur.

REFERENCES

1. Carmeliet, P., and Jain, R. K. (2011) Molecular mechanisms and clinical applications of angiogenesis. *Nature* **473,** 298–307
2. van Meeteren, L. A., and ten Dijke, P. (2012) Regulation of endothelial cell plasticity by TGF-β. *Cell Tissue Res.* **347,** 177–186
3. Goumans, M. J., Valdimarsdottir, G., Itoh, S., Lebrin, F., Larsson, J., Mummery, C., Karlsson, S., and ten Dijke, P. (2003) Activin receptor-like kinase (ALK)1 is an antagonistic mediator of lateral TGFβ/ALK5 signaling. *Mol. Cell* **12,** 817–828
4. Valdimarsdottir, G., Goumans, M. J., Rosendahl, A., Brugman, M., Itoh, S., Lebrin, F., Sideras, P., and ten Dijke, P. (2002) Stimulation of Id1 expression by bone morphogenetic protein is sufficient and necessary for bone morphogenetic protein-induced activation of endothelial cells. *Circulation* **106,** 2263–2270
5. Roelen, B. A., van Rooijen, M. A., and Mummery, C. L. (1997) Expression of ALK-1, a type 1 serine/threonine kinase receptor, coincides with sites of vasculogenesis and angiogenesis in early mouse development. *Dev. Dyn.* **209,** 418–430
6. Wu, X., Robinson, C. E., Fong, H. W., Crabtree, J. S., Rodriguez, B. R., Roe, B. A., and Gimble, J. M. (1995) Cloning and characterization of the murine activin receptor like kinase-1 (ALK-1) homolog. *Biochem. Biophys. Res. Commun.* **216,** 78–83
7. Seki, T., Hong, K. H., and Oh, S. P. (2006) Nonoverlapping expression patterns of ALK1 and ALK5 reveal distinct roles of each receptor in vascular development. *Lab. Invest.* **86,** 116–129
8. Urness, L. D., Sorensen, L. K., and Li, D. Y. (2000) Arteriovenous malformations in mice lacking activin receptor-like kinase-1. *Nat. Genet.* **26,** 328–331
9. Oh, S. P., Seki, T., Goss, K. A., Imamura, T., Yi, Y., Donahoe, P. K., Li, L., Miyazono, K., ten Dijke, P., Kim, S., and Li, E. (2000) Activin receptor-like kinase 1 modulates transforming growth factor-β1 signaling in the regulation of angiogenesis. *Proc. Natl. Acad. Sci. U.S.A.* **97,** 2626–2631
10. Park, S. O., Wankhede, M., Lee, Y. J., Choi, E. J., Fliess, N., Choe, S. W., Oh, S. H., Walter, G., Raizada, M. K., Sorg, B. S., and Oh, S. P. (2009) Real-time imaging of *de novo* arteriovenous malformation in a mouse model of hereditary hemorrhagic telangiectasia. *J. Clin. Investig.* **119,** 3487–3496
11. Niessen, K., Zhang, G., Ridgway, J. B., Chen, H., and Yan, M. (2010) ALK1 signaling regulates early postnatal lymphatic vessel development. *Blood* **115,** 1654–1661
12. Roman, B. L., Pham, V. N., Lawson, N. D., Kulik, M., Childs, S., Lekven, A. C., Garrity, D. M., Moon, R. T., Fishman, M. C., Lechleider, R. J., and Weinstein, B. M. (2002) Disruption of acvrl1 increases endothelial cell number in zebrafish cranial vessels. *Development* **129,** 3009–3019
13. Johnson, D. W., Berg, J. N., Baldwin, M. A., Gallione, C. J., Marondel, I., Yoon, S. J., Stenzel, T. T., Speer, M., Pericak-Vance, M. A., Diamond, A., Guttmacher, A. E., Jackson, C. E., Attisano, L., Kucherlapati, R., Porteous, M. E., and Marchuk, D. A. (1996) Mutations in the activin receptor-like kinase 1 gene in hereditary haemorrhagic telangiectasia type 2. *Nat. Genet.* **13,** 189–195
14. McAllister, K. A., Grogg, K. M., Johnson, D. W., Gallione, C. J., Baldwin, M. A., Jackson, C. E., Helmbold, E. A., Markel, D. S., McKinnon, W. C., and Murrell, J. (1994) Endoglin, a TGF-β binding protein of endothelial cells, is the gene for hereditary haemorrhagic telangiectasia type 1. *Nat. Genet.* **8,** 345–351
15. Castonguay, R., Werner, E. D., Matthews, R. G., Presman, E., Mulivor, A. W., Solban, N., Sako, D., Pearsall, R. S., Underwood, K. W., Seehra, J., Kumar, R., and Grinberg, A. V. (2011) Soluble endoglin specifically binds bone morphogenetic proteins 9 and 10 via its orphan domain, inhibits blood vessel formation, and suppresses tumor growth. *J. Biol. Chem.* **286,** 30034–30046
16. Blanco, F. J., Santibanez, J. F., Guerrero-Esteo, M., Langa, C., Vary, C. P., and Bernabeu, C. (2005) Interaction and functional interplay between endoglin and ALK-1, two components of the endothelial transforming growth factor-β receptor complex. *J. Cell. Physiol.* **204,** 574–584
17. van Meeteren, L. A., Goumans, M. J., and Ten Dijke, P. (2011) TGF-β receptor signaling pathways in angiogenesis; emerging targets for anti-angiogenesis therapy. *Curr. Pharm. Biotechnol.* **12,** 2108–2120
18. Mitchell, D., Pobre, E. G., Mulivor, A. W., Grinberg, A. V., Castonguay, R., Monnell, T. E., Solban, N., Ucran, J. A., Pearsall, R. S., Underwood, K. W., Seehra, J., and Kumar, R. (2010) ALK1-Fc inhibits multiple mediators of angiogenesis and suppresses tumor growth. *Mol. Cancer Ther.* **9,** 379–388
19. Cunha, S. I., Pardali, E., Thorikay, M., Anderberg, C., Hawinkels, L., Goumans, M. J., Seehra, J., Heldin, C. H., ten Dijke, P., and Pietras, K. (2010) Genetic and pharmacological targeting of activin receptor-like kinase 1 impairs tumor growth and angiogenesis. *J. Exp. Med.* **207,** 85–100
20. Kellermann, S. A., and Green, L. L. (2002) Antibody discovery: the use of transgenic mice to generate human monoclonal antibodies for therapeutics. *Curr. Opin. Biotechnol.* **13,** 593–597
21. Hu-Lowe, D., Wickman, G., Jiang, X., Kraynov, E., Wang, J., Amundson, K., Simmons, B., Liang, S., Chen, E., Karlicek, S., Thompson, J., Swanson, T., Yan, Z., Li, G., Los, G., Hostomsky, Z., Casperson, G., Bender, S., and North, M. (2009) in *Proceedings of the 100th Annual Meeting of the American Association for Cancer Research, Denver, April 18–22, 2009* (Abstr. 2007), American Association for Cancer Research, Philadelphia
22. Mancuso, P., Shalinsky, D. R., Calleri, A., Quarna, J., Antoniotti, P., Jilani, I., Hu-Lowe, D., Jiang, X., Gallo-Stampino, C., and Bertolini, F. (2009) Evaluation of ALK-1 expression in circulating endothelial cells (CECs) as an exploratory biomarker for PF-03446962 undergoing phase I trial in cancer patients. *J. Clin. Oncol.* **27,** 15s (suppl; abstr 3573)
23. Goff, L. W., De Braud, F. G., Cohen, R. B., Berlin, J., Noberasco, C., Borghaei, H., Wang, E., Hu-Lowe, D., Levin, W. J., and Gallo-Stampino, C. (2010) Phase I study of PF-03446962, a fully human mab against ALK1, a TGFβ receptor involved in tumor angiogenesis. *J. Clin. Oncol.* **28,** 15s (suppl; abstr 3034)
24. Persson, U., Izumi, H., Souchelnytskyi, S., Itoh, S., Grimsby, S., Engström, U., Heldin, C. H., Funa, K., and ten Dijke, P. (1998) The L45 loop in type I receptors for TGF-β family members is a critical determinant in specifying Smad isoform activation. *FEBS Lett.* **434,** 83–87
25. Korchynskyi, O., and ten Dijke, P. (2002) Identification and functional characterization of distinct critically important bone morphogenetic protein-specific response elements in the Id1 promoter. *J. Biol. Chem.* **277,**

4883–4891

26. Ebisawa, T., Tada, K., Kitajima, I., Tojo, K., Sampath, T. K., Kawabata, M., Miyazono, K., and Imamura, T. (1999) Characterization of bone morphogenetic protein-6 signaling pathways in osteoblast differentiation. *J. Cell Sci.* **112,** 3519 –3527

27. Nakatsu, M. N., Davis, J., and Hughes, C. C. (2007) Optimized fibrin gel bead assay for the study of angiogenesis. *J. Vis. Exp.* **3,** 186

28. Hughes, C. C. (2007) Christopher Hughes: an *in vitro* model for the study of angiogenesis (interview). *J. Vis. Exp.* **3,** 175

29. Frolik, C. A., Wakefield, L. M., Smith, D. M., and Sporn, M. B. (1984) Characterization of a membrane receptor for transforming growth factor-β in normal rat kidney fibroblasts. *J. Biol. Chem.* **259,** 10995–11000

30. Yamashita, H., ten Dijke, P., Huylebroeck, D., Sampath, T. K., Andries, M., Smith, J. C., Heldin, C. H., and Miyazono, K. (1995) Osteogenic protein-1 binds to activin type II receptors and induces certain activin-like effects. *J. Cell Biol.* **130,** 217–226

31. Scharpfenecker, M., van Dinther, M., Liu, Z., van Bezooijen, R. L., Zhao, Q., Pukac, L., Löwik, C. W., and ten Dijke, P. (2007) BMP-9 signals via ALK1 and inhibits bFGF-induced endothelial cell proliferation and VEGF-stimulated angiogenesis. *J. Cell Sci.* **120,** 964 –972

32. Goumans, M. J., Valdimarsdottir, G., Itoh, S., Rosendahl, A., Sideras, P., and ten Dijke, P. (2002) Balancing the activation state of the endothelium via two distinct TGF-β type I receptors. *EMBO J.* **21,** 1743–1753

33. David, L., Mallet, C., Keramidas, M., Lamandé, N., Gasc, J. M., Dupuis-Girod, S., Plauchu, H., Feige, J. J., and Bailly, S. (2008) Bone morphogenetic protein-9 is a circulating vascular quiescence factor. *Circ. Res.* **102,**

914 –922

34. Suzuki, Y., Ohga, N., Morishita, Y., Hida, K., Miyazono, K., and Watabe, T. (2010) BMP-9 induces proliferation of multiple types of endothelial cells *in vitro* and *in vivo. J. Cell Sci.* **123,** 1684 –1692

35. Scotti, C., Olivieri, C., Boeri, L., Canzonieri, C., Ornati, F., Buscarini, E., Pagella, F., and Danesino, C. (2011) Bioinformatic analysis of pathogenic missense mutations of activin receptor like kinase 1 ectodomain. *PLoS One* **6,** e26431

36. David, L., Mallet, C., Mazerbourg, S., Feige, J. J., and Bailly, S. (2007) Identification of BMP9 and BMP10 as functional activators of the orphan activin receptor-like kinase 1 (ALK1) in endothelial cells. *Blood* **109,** 1953–1961

37. Brown, M. A., Zhao, Q., Baker, K. A., Naik, C., Chen, C., Pukac, L., Singh, M., Tsareva, T., Parice, Y., Mahoney, A., Roschke, V., Sanyal, I., and Choe, S. (2005) Crystal structure of BMP-9 and functional interactions with pro-region and receptors. *J. Biol. Chem.* **280,** 25111–25118

38. Larrivée, B., Prahst, C., Gordon, E., Del Toro, R., Mathivet, T., Duarte, A., Simons, M., and Eichmann, A. (2012) ALK1 signaling inhibits angiogenesis by cooperating with the Notch pathway. *Dev. Cell* **22,** 489 –500

39. Seehra, J., Knopf, J., Pearsall, R. S., Grinberg, A., and Kumar, R. (November 19, 2009) International Patent WO2009139891

40. North, M. A., Amundson, K. K., Bedian, V., Belouski, S. S., Hu-Lowe, D. D., Jiang, X., Karlicek, S. M., Kellermann, S.-A., Thomson, J. A., Wang, J., Wickman, G. R., and Zhang, J. (April 21, 2007) International Patent WO2007040912